Cortactin, an 80/85-Kilodalton pp60^{src} Substrate, Is a Filamentous Actin-binding Protein Enriched in the Cell Cortex

Hong Wu and J. Thomas Parsons

Department of Microbiology and Cancer Center, University of Virginia Health Sciences Center, Charlottesville, Virginia 22908

Abstract. Two related cellular proteins, p80 and p85 (cortactin), become phosphorylated on tyrosine in pp60^{src}-transformed cells and in cells stimulated with certain growth factors. The amino-terminal half of cortactin is comprised of multiple copies of an internal, tandem 37-amino acid repeat. The carboxyl-terminal half contains a distal SH3 domain. We report that cortactin is an F-actin-binding protein. The binding to F-actin is specific and saturable. The amino-terminal repeat region appears to be both necessary and sufficient to mediate actin binding, whereas the SH3 domain had no apparent effect on the actin-binding activity. Cortactin, present in several different cell types, is enriched in cortical structures such as membrane ruffles and lamellipodia. The properties of cortactin indicate that it may be important for microfilament-membrane interactions as well as transducing signals from the cell surface to the cytoskeleton. We suggest the name cortactin, reflecting the cortical subcellular localization and its actin-binding activity.

Cells undergo structural rearrangement during cell division, cell migration, oncogenic transformation, and in response to stimulation with a variety of extracellular ligands (Albert et al., 1989). Vertebrate cells exhibit a cortical cytoskeletal network that resides beneath, and is associated with, the inner surface of the plasma membrane (Bray et al., 1986). This cortical cytoskeleton is comprised of a dense network of actin filaments and associated actin-binding proteins (Small et al., 1981; Stossel et al., 1981). Components of both the cell cortex and the plasma membrane are important for the integration of cell surface signals, facilitating transfer of these signals to the interior of the cell. The alterations in cortical cytoskeleton accompany a variety of cellular processes, including phagocytosis, cytokinesis, cell locomotion, cell-cell and cell-substratum interaction, transmembrane signaling, secretion, and endocytosis (for reviews see Tilney, 1983; Albert et al., 1989; Bretscher, 1991).

The structure and physical properties of the cortical cytoskeleton are determined, in large part, by cooperative and competitive interactions among many actin-binding proteins (Albert et al., 1989). Based on both in vitro and in vivo studies, a large number of actin-binding proteins have been identified that control assembly and length of actin filaments, link actin filaments into bundles or networks, define the three-dimensional organization of actin filaments and link filaments to other cytoplasmic and membrane components (for reviews see Stossel et al., 1985; Pollard and Cooper, 1986; Albert et al., 1989; Stossel, 1989; Vandekerckhove, 1990; Hartwig and Kwiatkowski, 1991). Subcellular localization studies have shown that many of the actin-binding proteins, such as filamin, villin, gelsolin , and ezrin, are enriched in the submembranous cortical region (Bretscher, 1991). In addition, the interaction of many actin-binding proteins with either monomeric actin or filamentous actin (F-actin)[1] is regulated by common intracellular signals, including calcium, calmodulin, phospholipids, and protein phosphorylation (Vandekerckhove, 1990; Yamashiro et al., 1990; Hartwig et al., 1992). Studies on the regulation of gelsolin and profilin by Ca^{2+} and phosphatidylinositides have provided models for the reorganization of actin filament network (Stossel, 1989). In vivo studies have documented changes in the activity of certain actin-binding proteins concomitant with cellular events such as receptor stimulation and mitosis (Yamashiro et al., 1990; Goldschmidt-Clermont et al., 1991; Hartwig et al., 1992). The functional significance of actin-binding proteins is further emphasized by the diverse phenotypes exhibited in cell lines or transgenic organisms which either lack or overexpress actin-binding proteins (for review see Noegel and Schleicher, 1991).

Cellular transformation by oncogenic tyrosine kinases is characterized by overt changes in cellular growth control and dramatic changes in cell morphology and cell surface topology (for reviews see Jove and Hanafusa, 1987; Parsons and Weber, 1989). Chicken embryo (CE) cells transformed by pp60^{src}, the oncogenic tyrosine kinase encoded by Rous sarcoma virus, are morphologically round. This phenotype is accompanied by loss of actin stress fibers and aggregation of F-actin into podosomes (David-Pfeuty and Singer, 1980;

1. *Abbreviations used in this paper*: CE, chicken embryo; F-actin, filamentous actin; GST, glutathione-*S*-transferase.

© The Rockefeller University Press, 0021-9525/93/03/1417/10 $2.00

Tarone et al., 1985; Holme et al., 1986; Marchisio et al., 1987). The importance of the cytoskeleton in cellular transformation by protein tyrosine kinase oncogenes has been supported by the study of *src* mutants. The transforming activity of the various pp60^{src} mutants correlates with the degree of their association with detergent-insoluble cytoskeleton elements (Hamaguchi and Hanafusa, 1987). The study of cellular substrates of pp60^{src} has also pointed to the involvement of cytoskeletal proteins in the process of cellular transformation and cell signaling (for reviews see Hunter, 1989; Schaller et al., 1993*b*). Several newly characterized pp60^{src} substrates are either cytoskeletal proteins or associated with the cytoskeleton. These include FAK, a focal adhesion protein tyrosine kinase (Schaller et al., 1992); pp120, a tyrosine-phosphorylated protein that shares sequence similarity with plakoglobin and *armadillo* (Kanner et al., 1991*a*; Reynolds et al., 1992); pp110, a phosphotyrosine-containing protein that localizes to stress fibers in CE cells (Kanner et al., 1991*b*; Flynn, D. C., and J. T. Parsons, manuscript in preparation); tensin, an F-actin capping and bundling protein (Davis et al., 1991); p22 caveolin, a coating protein for nonclathrin-coated pits (Glenney and Zokas, 1989; Rothberg et al., 1992); and paxillin, a focal adhesion protein associated with vinculin (Turner et al., 1990).

Recently, we reported the identification of two proteins, designated p80/85, which are substrates for activated pp60^{src} protein tyrosine kinase (Wu et al., 1991). p80/85 is also tyrosine phosphorylated in cells stimulated with EGF, PDGF, colony stimulating factor I (Downing and Reynolds, 1992; Maa et al., 1992), and in platelets stimulated with thrombin (Wong et al., 1992; Lipfert, L., and J. S. Brugge, personal communication). p80/85 exhibits several unique structural features. The amino-terminal half of the protein is comprised of multiple copies of an internal, tandem 37-amino acid repeat (referred to as "repeat region"). The number of repeat units appears to be specified by alternative splicing since, in CE cells, cDNAs have been identified that encode proteins with five (p80) or six copies (p85) of the tandem repeat (Hildebrand, J. D., and J. T. Parsons, manuscript in preparation). The carboxyl-terminal half of the protein contains a distal SH3 (*src* homology 3) domain, preceded by a region of 50 amino acids with a predicted helical structure and a region rich in proline, serine, and threonine. Here we report that p80/85 protein is an F-actin-binding protein. The binding to F-actin is specific and saturable. The amino-terminal repeat region of the protein appears to be both necessary and sufficient to mediate actin binding. Deletions removing the SH3 domain, the helical region, and the proline/serine/threonine region, had no apparent effect on the actin-binding activity. p80/85 is present in several different cell types and in each is enriched in cortical structures such as membrane ruffles and lamellipodia. The submembranous location of p80/85 indicates that the protein may be important for microfilament-membrane interaction as well as transducing signals from the cell surface to the cytoskeleton. Based on the cortical localization and actin-binding properties of p80/85, we propose the name "cortactin."

Materials and Methods

Preparation of Cell Extracts

Primary CE cells were prepared from 10-d embryos (SPAFAS Inc., Norwich, CT). CE cells were transformed by transfecting cells with plasmid DNA containing the activated *c-src* gene, *c-src*527F, as described previously (Reynolds et al., 1989). Both normal and transformed CE cells were maintained in DME with 5% FBS. CE cells were lysed by incubating cells with ice-cold G-buffer (2 mM Tris-HCl [pH 8], 0.2 mM ATP, 0.5 mM DTT, and 0.2 mM $CaCl_2$) for 15 min, followed by 30 strokes with a tight-fitting Dounce homogenizer. Cell lysates were clarified by centrifugation at 10,000 *g* for 10 min. The proteins were subjected to SDS-PAGE analysis, and immunoblotted with either 5 μg/ml of purified anticortactin mAbs (4F11 or 1H3) or affinity-purified rabbit phosphotyrosine antibodies, as previously described (Wu et al., 1991).

F-actin Cosedimentation Assay

Rabbit muscle actin was purified as described (Pardee and Spudich, 1982). The purity of the actin preparation was assessed by SDS-PAGE and Coomassie blue staining. Typically, actin preparations were >90-95% pure, as judged by the relative staining of a 43-kD actin band. Purified actin was stored in G-buffer. Actin was polymerized by adjusting the buffer condition to that of F-buffer (2 mM Tris-HCl [pH 8], 0.2 mM DTT, 0.2 mM $CaCl_2$, 50 mM KCl, 2 mM $MgCl_2$, and 1 mM ATP).

F-actin cosedimentation assays were performed by mixing either 50 μl CE cel lysate, 5-10 μl of in vitro translation products, or 0.5-17 μg of glutathione-*S*-transferase (GST) fusion protein with 15-30 μg of polymerized actin. The mixture (55-100 μl) was incubated on ice for 1 h, and then layered over 50 μl of 10% sucrose in F-buffer and centrifuged for 15 min or 1 h at 100,000 *g* at 4°C in a Ti42.2 rotor (Beckman Instruments, Inc., Fullerton, CA) (Pope and Weeds, 1986; Hug et al., 1992). After removal of the supernatant, the pellet was incubated for at least 1 h with 50 μl of G-buffer at 4°C, and then solubilized in hot sample buffer (Laemmli, 1970). The supernatant and pellet fractions were fractionated by SDS-PAGE, analyzed either by immunoblotting with anticortactin mAbs, fluorography, or by Coomassie blue staining. For mAb inhibition of cortactin binding to F-actin, CE lysates were preincubated with individual anticortactin mAbs (1-3 μg mAb/100 μg cell protein) on ice for 1 h before mixing the lysate with F-actin.

To assess the binding of GST.p80 fusion protein, 0.5-17 μg of purified fusion protein was incubated with 15 μg of polymerized actin in a total volume of 75 μl. The cosedimentation assay was performed as described above. The pellet was washed three times with F-buffer before solubilization. Supernatant and solubilized pellet fractions were fractionated by SDS-PAGE and stained with Coomassie blue. To quantitate the amount of fusion protein, several different concentrations of BSA were included in the same gel to serve as internal protein concentration standards. The stained BSA and fusion protein bands were quantitated using a Visage 4000 (BioImage, Ann Arbor, MI) in combination with whole band analysis software. The data were analyzed using GraphPad Inplot, version 4.0 (Graph Pad Software for Sci., San Diego, CA).

Construction of Plasmids Encoding GST Fusion Proteins and Fusion Protein Preparation

A cDNA encoding the 80-kD form of cortactin was subcloned into pBluescript vector (Stratagene, La Jolla, CA). Restriction enzyme fragments containing different coding regions of p80 were subcloned into a pGex vector (Fig. 1), in frame with sequences encoding the GST (Smith and Johnson, 1988). GST.p80 was constructed using a BamHI-EcoRI fragment of p80 cDNA, containing amino acid residues 55-526; GST.55-292 contains a BamHI-BsmI fragment and GST.294-526 contains a BsmI-EcoRI fragment, encoding amino acid residues 55-292 and 294-526, respectively.

The induction of fusion proteins was performed as described by Smith and Johnson (1988). The bacteria were resuspended in MTPBS buffer (150 mM NaCl, 16 mM Na_2HPO_4, 4 mM NaH_2PO_4, pH 7.3) containing 1 mM PMSF, 0.1 mM DTT, 10 mM EDTA, and 50 μg/ml leupeptin. Cells were lysed by sonication after addition of Triton X-100 to 1%. The cell lysate was clarified by centrifugation at 10,000 *g* for 10 min. 50-100 μl of the supernatant was mixed with 20-40 μl of 50% glutathione Sepharose 4B beads (Pharmacia, Uppsala, Sweden) at room temperature for 5 min. The beads were washed three times with MTPBS and the GST fusion protein was eluted by mixing the beads with 20 mM glutathione, 50 mM Tris-HCl, pH 7.5 at room temperature for 5 min. The elution was repeated. The eluted material was pooled and used for further experiments. The fusion proteins were analyzed by SDS-PAGE, detected either by Coomassie blue staining or by immunoblotting with anticortactin mAbs.

For large-scale preparation of the GST fusion proteins, overnight cultures

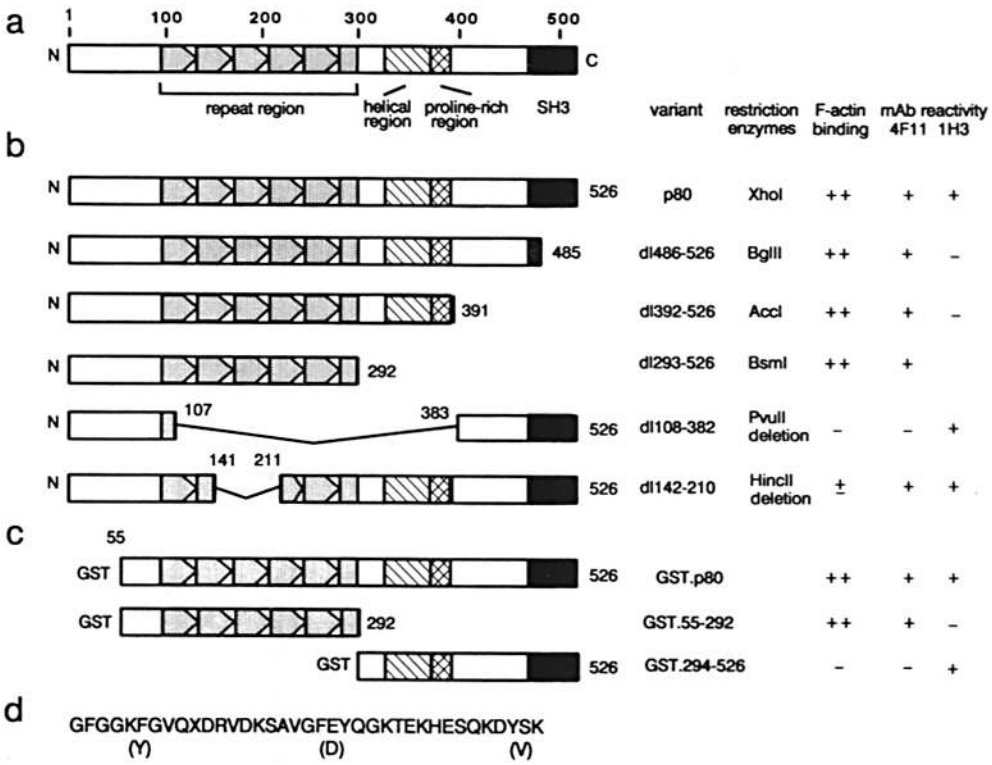

Figure 1. Diagrammatic representation of cortactin and cortactin variants. (*a*) Diagram of cortactin structure. The internal repeats are indicated by the dotted region, and the SH3 domain is shown by the filled region. The predicted α-helical and the adjacent Pro-, Ser-, and Thr-rich region are denoted by the stripped and crosshatched boxes, respectively. (*b*) Diagram of in vitro-translated cortactin. For 3' truncations, cortactin cDNA was cleaved with the restriction enzymes indicated at the right (the restriction enzyme XhoI cleaves within the pBluescript polylinker sequence). Internal deletions were generated by in-frame ligation of the indicated restriction fragments. Each individual cDNA construct was used as DNA template for in vitro transcription–translation reactions as discussed in Materials and Methods. (*c*) Diagram of GST–cortactin fusion proteins. Different portions of the cortactin cDNA were fused in-frame with GST in the pGex vector, and fusion proteins were expressed and isolated as discussed in Materials and Methods. The F-actin–binding activity and immunoreactivity with mAbs (4F11 or 1H3) of individual constructs are listed at the right. The numbers in the diagram indicate amino acid residues. (*d*) Consensus amino acid sequence of the repeat region of cortactin. The consensus sequence denotes identical amino acid residues that are present in at least three of the five complete repeats in p80 of cortactin. Amino acid residues that are present in two of the five repeats are shown in parentheses. Letter *x* represents position where no common residue was present.

were diluted 1:10 into 500 ml of LB media, grown for 1 h, and induced with 0.2 mM isopropyl-β-thiogalactopyniroside for an additional 2 h. Bacteria were resuspended in 20 ml MTPBS and sonicated as described. The lysate was centrifuged at 10,000 *g* for 10 min at 4°C. The supernatant was mixed with 1 ml of glutathione beads at 4°C for 1 h with rocking. The beads were washed three times with MTPBS and the fusion proteins were eluted by mixing the beads with 1 ml of the same elution buffer at room temperature for 2 min (Smith and Johnson, 1988; Hug et al., 1992).

In Vitro Transcription and Translation

A cDNA clone of the 80-kD form of cortactin in pBluescript was digested with individual restriction enzymes as indicated in Fig. 1. Messenger RNAs were transcribed from individual DNA templates using an mRNA capping kit (Stratagene, La Jolla, CA) containing T7 DNA polymerase and a 7-methylguanosine CAP analog. 5 μg of template DNA was used per 50-μl reaction. Translation was carried out in a rabbit reticulocyte lysate (Promega Corp., Madison, WI or Stratagene). A typical 50-μl translation reaction contained 25 μl reticulocyte lysate, 40 μCi [^{35}S]methionine (1,139 Ci/mmol, Dupont, NEN Research Products, Boston, MA), and ~20% of the heat-denatured RNA from a single transcription reaction. The reaction mixture was incubated at 30°C for 60 min and 5–10-μl aliquots were used for F-actin cosedimentation assays (Neri et al., 1991). Labeled translation products were resolved by 10% SDS-PAGE and detected by fluorography.

Immunofluorescence Microscopy

Immunofluorescence microscopy was carried out as previously described (Wu et al., 1991). Cells were seeded and grown overnight on glass coverslips, washed with PBS, fixed, and permeabilized. Permeabilized cells were incubated with primary anticortactin mAbs and then with rabbit anti-mouse IgG, and detected with FITC-conjugated donkey anti-rabbit IgG as previously described (Wu et al., 1991). For double immunostaining experiments, cells were also incubated with rhodamine-phalloidin as previously described (Wu et al., 1991). Samples were visualized with a Leitz Orthoplan fluorescence microscope. For cytochalasin D treatment, cells were incubated with 2 μM cytochalasin D in growth media for 15 min at 37°C before fixation (Cooper, 1987).

Results

Localization of Cortactin to the Cell Cortex

Previous experiments have shown that p80/85 or cortactin colocalizes with F-actin in the peripheral extensions of normal cells and podosomes (rosettes) of pp60^{src}-transformed cells (Wu et al., 1991). Indirect immunofluorescence of spreading CE cells using anticortactin mAbs revealed intense staining of cortical structures such as the membrane ruffles and lamelliopodia (Fig. 2, *a* and *b*). The same staining pattern was observed in several other adherent cell types, including rat aortic smooth muscle cells and rat endothelial cells (Fig. 2, *c* and *d*). The staining pattern is very similar to that of cortical actin as judged by costaining experiments with phalloidin (data not shown). Cells incubated with the microfilament disrupting agent cytochalasin D exhibited a dramatic alteration in the staining pattern of cortactin. The resulting cytoplasmic aggregates of cortactin colocalized with F-actin aggregates, as demonstrated by costaining of the cells with anticortactin mAb and phalloidin (Fig. 2, *e* and *f*). The result of such immunostaining experiments indicated a colocalization of cortactin with F-actin and suggested a possible direct interaction of cortactin with F-actin.

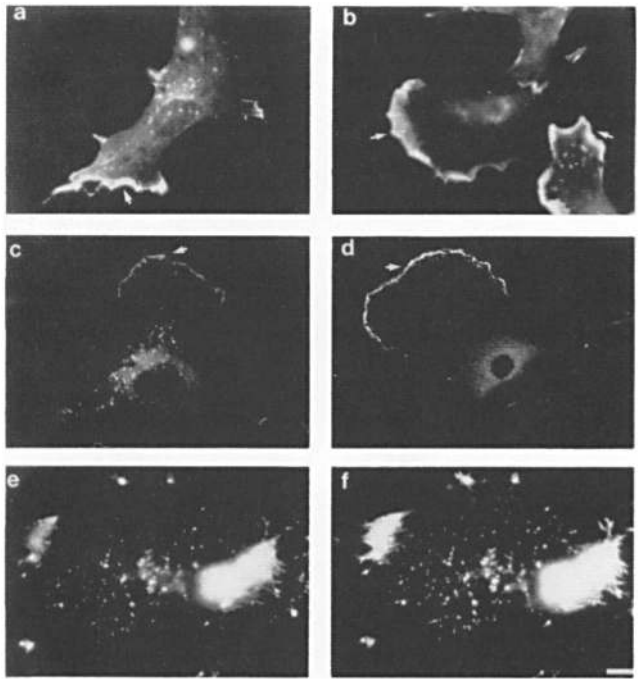

Figure 2. Immunostaining of cortactin. CE cells (*a* and *b*), rat aortic smooth muscle cells (*c*), and rat endothelial cells (*d*) were grown overnight on glass coverslips, fixed, and immunostained with mAb 4F11 as described in Materials and Methods. In *e* and *f*, CE cells were pretreated with cytochalasin D before fixation, and then costained with mAb 4F11 (*e*) and rhodamine-phalloidin (*f*). Arrows in *a–d* denote intense staining of the cell cortex. Bar, 10 μm.

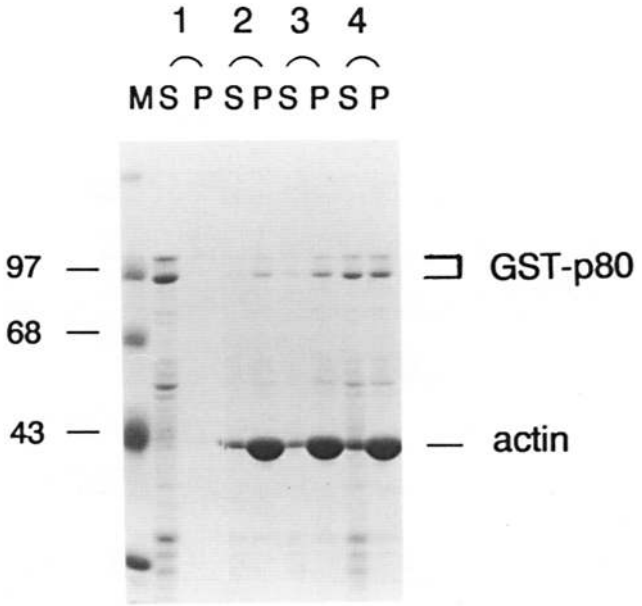

Figure 4. Interaction of GST-cortactin fusion protein with F-actin. GST.p80 fusion protein was constructed and purified as described in Materials and Methods. 3 μg (lanes *2*), 5 μg (lanes *3*), and 7 μg (lanes *4*) of purified GST.p80 was incubated with F-actin, and the mixture was centrifuged. Supernatant (lanes *S*) and pellet (lanes *P*) were resolved by SDS-PAGE and stained with Coomassie blue. As a control, an aliquot of GST.p80 fusion protein was centrifuged without preincubation with F-actin (lanes *1*). The position of the GST.p80 fusion protein and the major proteolytic product as well as actin are indicated. Molecular mass markers are shown in lane *M* and the sizes are indicated at the left in kD.

Binding of Cortactin to F-actin

To test the possible binding of cortactin to F-actin, CE cell lysates were incubated with polymerized rabbit muscle actin and an F-actin cosedimentation assay was carried out. After sedimentation of F-actin, >95% of the cortactin present in the cell lysate cosedimented with F-actin (Fig. 3, *a*, lanes *2* and *3*). In the absence of F-actin, cortactin remained in the supernatant fraction (Fig. 3, *a*, lanes *1*). As shown in *b*, the majority of the F-actin sedimented to the pellet fraction under conditions of the assay, indicating a quantitative polymerization of the monomeric actin. In control incubations, BSA, which does not have actin-binding activity, remained in the supernatant fraction (Fig. 3 *b*, lanes *3*). Similar binding of cortactin to F-actin was observed when purified chicken muscle F-actin was used in the assay (data not shown).

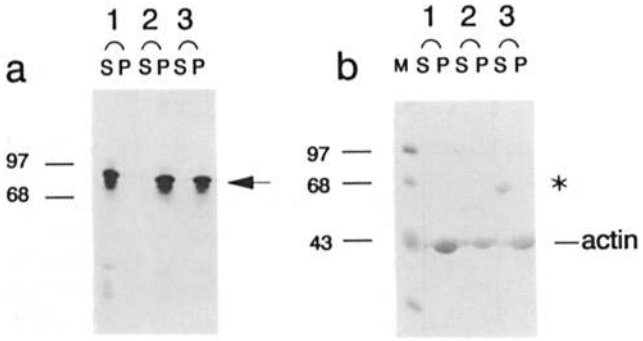

Figure 3. Cosedimentation of cortactin with F-actin. 50 μl of CE cell lysates, prepared as described in Materials and Methods, were incubated with either 15 μg (*a*, lanes *2*; *b*, lanes *1*) or 7 μg (*a*, lanes *3*; *b*, lanes *2*) of rabbit muscle F-actin, and the mixture was centrifuged. Aliquots of supernatant (lanes *S*) and pellet (lanes *P*) were resolved by SDS-PAGE. Equal amounts of the samples were either immunoblotted with mAb 4F11 (panel *a*) or stained with Coomassie blue (*b*). As controls, CE cell lysate without F-actin was centrifuged (*a*, lanes *1*); 10 μg BSA was mixed with F-actin and centrifuged (*b*, lanes *3*). The positions of the major bands of cortactin and BSA are denoted by arrow and star, respectively. Molecular mass markers are shown in lane *M*, and the sizes are indicated at the left in kD.

The results of the cosedimentation assay indicated that cortactin, present in CE cell lysates, may bind directly to F-actin. To further test this hypothesis, [^{35}S]methionine-labeled cortactin, synthesized by in vitro translation of cortactin mRNA in a reticulocyte lysate, was used in an F-actin cosedimentation assay. A significant portion of the in vitro-translated 80-kD form of cortactin cosedimented with F-actin, providing evidence for the direct interaction of cortactin with F-actin (see Fig. 6, lanes *1b*).

Since it was possible that the interaction of cortactin with F-actin might be mediated through a cellular component present in either the CE cell lysate or the reticulocyte lysate, cortactin was expressed as a GST fusion protein in *Escherichia coli* and its actin-binding properties were investigated. The GST.p80 fusion protein contains amino acid residues 55–526 of p80 fused in frame to sequences encoding GST. As shown in Fig. 4 (lanes *2*), the purified GST.p80 protein

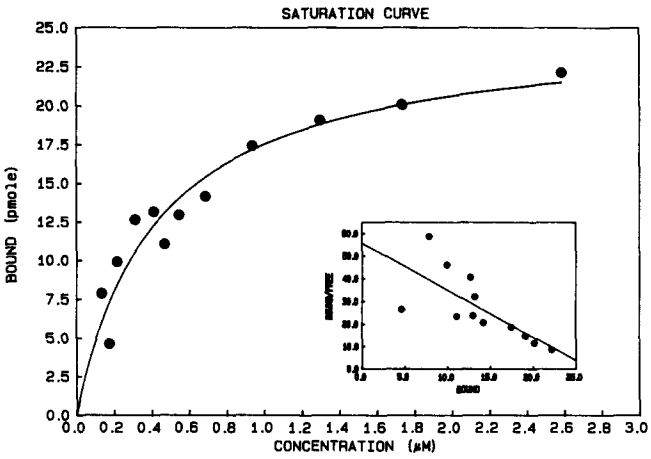

Figure 5. Binding curve of cortactin to F-actin. Different amounts of purified GST.p80 fusion protein were incubated with 15 μg of F-actin and the mixture was centrifuged, as described in Materials and Methods. Supernatant and pellet fractions were resolved by SDS-PAGE and stained with Coomassie blue (as in Fig. 4). The concentrations of bound and free fusion protein were determined by quantitation of individual bands on a densitometer. The curve represents a theoretical binding isotherm for $K_d = 0.43 \pm 0.08$ μM. The inset shows a Scatchard analysis of the same data.

cosedimented with F-actin. Moreover, addition of increasing amounts of GST.p80 protein to a fixed amount of F-actin in the cosedimentation assay revealed that the binding of cortactin to F-actin was saturable (Fig. 4, lanes *3* and *4*). Best fit analysis of the binding data indicated the presence of a single binding site (Fig. 5). At saturation, the binding stoichiometry is ~1 GST.p80 protein per 14 actin monomers (Fig. 5). Taken together, these data demonstrate that cortactin from three different sources binds efficiently to F-actin, providing evidence that cortactin interacts directly with F-actin.

Mapping of F-actin Binding Site to Repeat Region of Cortactin

The specificity of the interaction of cortactin with F-actin was further assessed by mapping the region of cortactin that is necessary for the binding. [^{35}S]Methionine-labeled cortactin was synthesized by directing in vitro transcription-translation reactions with individual p80 cDNA constructs, illustrated in Fig. 1 *b*. To generate a series of carboxyl-terminal truncated cortactin molecules, p80 cDNAs were digested with restriction enzymes that cleave within the 3′ portion of the coding sequence (Fig. 1 *b*). Internal deletions were created by in-frame ligation of p80 cDNA fragments generated by cleavage with specific restriction enzymes (Fig. 1 *b*). Binding to F-actin was tested in an F-actin cosedimentation assay (Fig. 6). Truncated cortactin, lacking the SH3 domain (dl486–526 and dl392–526, lanes *2b* and *3b*) or lacking the carboxyl-terminal half of the protein (dl293–526, lanes *6b*) cosedimented with F-actin, mimicking the activity of the full-length protein (lanes *1b*). In contrast, an internal deletion of amino acid residues 108–382, which deleted the complete repeat region, as well as the following helical region and most of the proline-rich region (Fig. 1 *b*), did not cosediment with F-actin (Fig. 6, lanes *5b*). A cortactin variant, with a smaller internal deletion which removed amino acid residues 142–210 within the repeat region, showed a significantly decreased binding to F-actin (lanes *4b*). These results indicated that the amino acid sequences comprising the carboxyl-terminal half of the protein, including the SH3 domain, were not required for the binding of cortactin to F-actin. Instead, the tandemly repeated sequences comprising the repeat region appeared to be necessary for the efficient binding of cortactin to F-actin.

To assess which sequences of cortactin were sufficient to reconstitute the F-actin binding activity, the amino- and carboxyl-terminal halves of p80 were fused separately to GST and expressed as GST fusion proteins in *E. coli*.

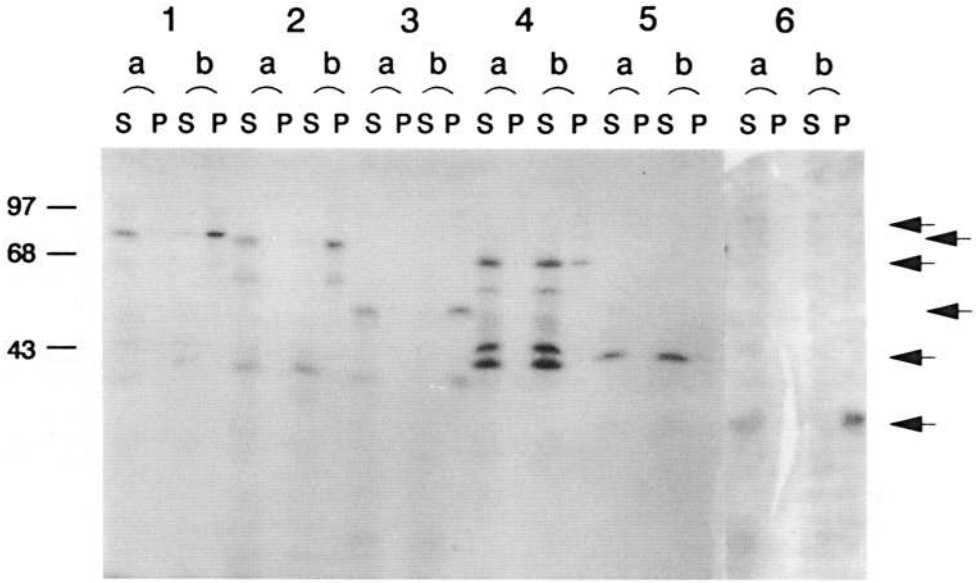

Figure 6. Binding of in vitro-truncated cortactin with F-actin. [^{35}S]Methionine-labeled proteins were synthesized in vitro using various cortactin cDNA constructs (diagrammed in Fig. 1 *b*). An aliquot of each translation product was incubated with F-actin and the mixture was centrifuged (lanes *b*). As controls, the same amount of the translation products was centrifuged without preincubation with F-actin (lanes *a*). Supernatant (lanes *S*) and pellet (lanes *P*) were resolved by SDS-PAGE and the proteins detected by fluorography. (Lanes *1*) Translation product of the full-length cortactin cDNA; (lanes *2*) dl486–526; (lanes *3*) dl392–526; (lanes *4*), dl108–382; (lanes *5*) dl142–210; and (lanes *6*) dl293–526. Positions of the specific translation products are indicated by arrow. In each lane, the smaller radiolabeled proteins detected in the individual lanes likely represent prematurely terminated translation products, since they are absent from unprogrammed lysates. Molecular mass markers are indicated in kD.

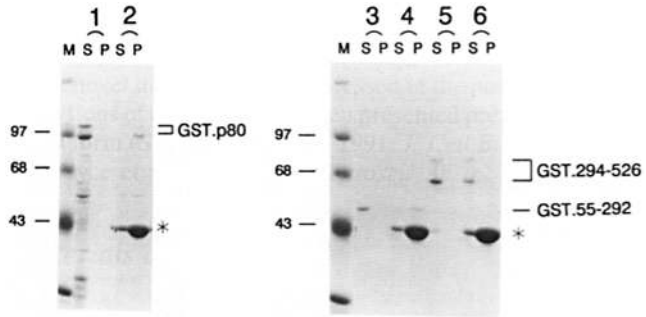

Figure 7. Interaction of GST–cortactin fusion proteins with F-actin. Purified GST fusion proteins (illustrated in Fig. 1 *c*) were either preincubated with F-actin and centrifuged (lanes *2*, *4*, and *6*) or centrifuged alone (lanes *1*, *3*, and *5*). Supernatant (lanes *S*) and pellet (lanes *P*) were separated by SDS-PAGE and stained with Coomassie blue. (Lanes *1* and *2*) GST.p80; (lanes *3* and *4*) GST.55–292; (lanes *5* and *6*) GST.294–526. The positions of the fusion proteins and the major proteolytic product are indicated. The molecular mass markers are shown in lanes *M* and the sizes are indicated at the left in kD.

GST.55–292 and GST.294–526 contain, respectively, amino acid residues 55–292 and 294–526 (Fig. 1 *c*). As shown in Fig. 7, GST.55–292 cosedimented with F-actin, whereas the majority of GST.294–526 remained in the supernatant. These results confirmed that the repeat region of cortactin participated in F-actin binding and indicated that this region may be sufficient for the binding. Although the repeat region appears to be both necessary and sufficient for F-actin binding, we cannot rule out the possibility that there are other weaker actin-binding sites. The small amount of GST.294–526 observed in the pellet fraction may be indicative of such a site in the carboxyl-terminal half of the protein (lanes *6*).

Inhibition of Cortactin–F-actin Interaction with mAbs

As previously reported, several mAbs appear to interact with different epitopes within cortactin (Wu et al., 1991). Four different mAbs were tested for their ability to inhibit the binding of cortactin to F-actin (Fig. 8). Preincubation of cell lysates with anticortactin mAb 4F11 before mixing with F-actin blocked the association of cortactin with F-actin (Fig. 8, lanes *3* and *4*). In contrast, preincubation of cell lysates with either mAb 1H3 (lanes *6*), mAb 3B12, or 3D9 (data not shown) did not affect the cosedimentation of cortactin with F-actin. To better understand the nature of the mAb inhibition, we mapped the epitopes of mAb 4F11 and 1H3. GST fusion proteins containing portions of cortactin were tested for their reactivity with the two mAbs in a Western blot. As shown in Fig. 9, mAb 4F11 reacted with GST.p80 (lane *1*) as well as GST.55–292 (lane *2*), but not with GST.294–526 (lane *3*). Conversely, mAb 1H3 reacted with GST.p80 (lane *4*) and GST.294–526 (lane *6*), but not with GST.55–292 (lane *5*). This localized the binding sequences for 4F11 and 1H3 to the amino-terminal half and the carboxyl-terminal half of the protein, respectively. The epitopes for 4F11 and 1H3 were further mapped by immunoprecipitation of the individual, in vitro-translated cortactin proteins (summarized in Fig. 1). A cortactin variant with a deletion of amino acid residues 108–382 was not immunoprecipitated by mAb 4F11, whereas variants with a deletion of amino acid residues 142–210 or lacking the carboxyl-terminal region were readily im-

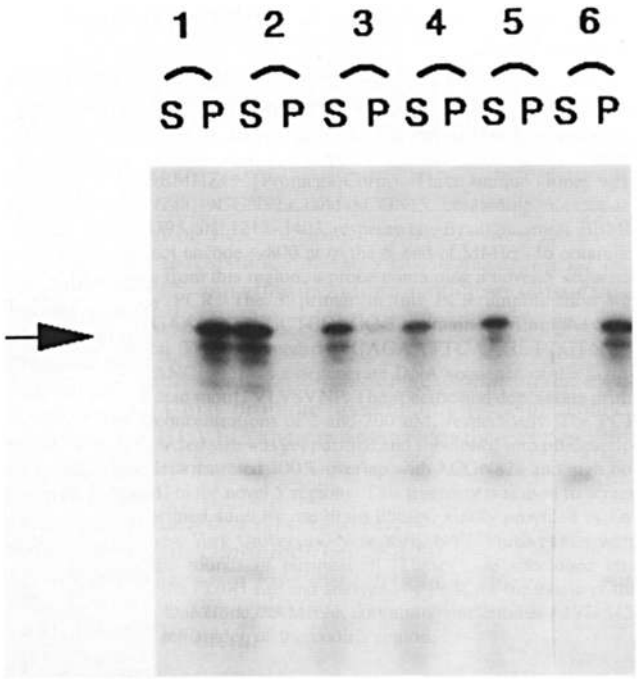

Figure 8. Inhibition of cortactin binding to F-actin by anticortactin mAb. CE cell lysate (lanes *1*) and lysates pretreated with mAb 4F11 (lanes *2–4*) or mAb 1H3 (lanes *5* and *6*) were either incubated with F-actin and centrifuged (lanes *1*, *3*, *4*, and *6*) or centrifuged alone (lanes *2* and *5*). Supernatant (lanes *S*) and pellet (lanes *P*) were resolved by SDS-PAGE, transferred to nitrocellulose, and immunoblotted with mAb 4F11. The arrow denotes the position of the major bands of cortactin.

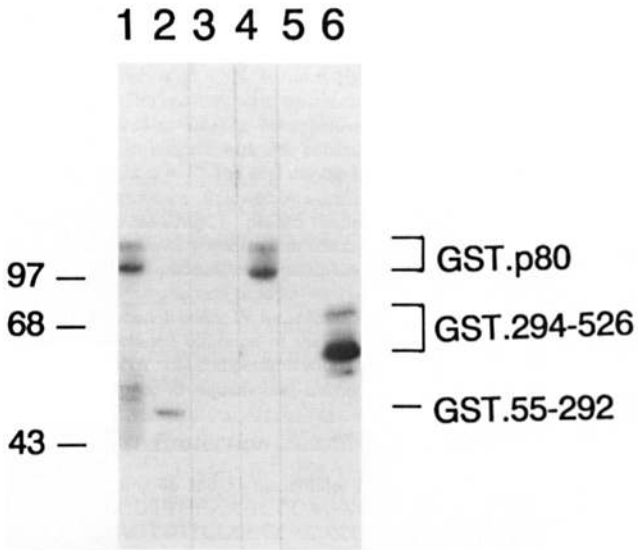

Figure 9. Mapping of epitopes of anticortactin mAbs. Purified GST.p80 (lanes *1* and *4*), GST.55–292 (lanes *2* and *5*), and GST.294–526 (lanes *3* and *6*) were resolved by SDS-PAGE, transferred to nitrocellulose, and immunoblotted with either mAb 4f11 (lanes *1–3*) or mAb 1H3 (lanes *4–6*). The positions of the fusion proteins and the major proteolytic product are indicated. Molecular mass markers are indicated in kD.

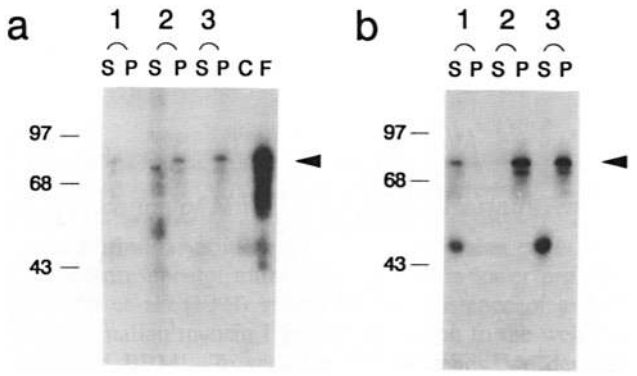

Figure 10. Binding of tyrosine-phosphorylated cortactin with F-actin. Lysates from pp60^{src}-transformed CE cells were incubated with F-actin and centrifuged (lanes *2* and *3*). Supernatant (lanes *2S*) and pellet (lanes *P*) were separated by SDS-PAGE, transferred to nitrocellulose, and immunoblotted with either phosphotyrosine antibodies (*a*) or mAb 4F11 (*b*). As controls, the same amount of cell lysates were centrifuged without F-actin (lanes *1*). In lanes *1S* and *3S*, the supernatant fractions were immunoprecipitated with mAb 4F11 and the immunocomplexes were resolved by SDS-PAGE and immunoblotted with either phosphotyrosine antibodies (*a*) or mAb 4F11 (*b*). In *a*, lysates from CE cells (lane *C*) or pp60^{src}-transformed CE cells (lane *F*) were also resolved by SDS-PAGE and immunoblotted with phosphotyrosine antibodies. The position of the major cortactin bands is indicated by an arrowhead. Molecular mass markers are indicated in kD.

munoprecipitated with mAb 4F11. These data indicated that the amino acid sequences within the regions of residues 211–383 or 107–141 were required for recognition by mAb 4F11. In light of the fact that 4F11 immunoblotted GST.55–292 which contains amino acid residues 55–292, it is likely that the 4F11 epitope resides within the repeat region of cortactin. Truncated cortactin molecules lacking the carboxyl-terminal 40 amino acid residues were not immunoprecipitated by mAb 1H3, mapping the 1H3 epitope to the SH3 domain of cortactin. In summary, the species cross-reactive mAb 4F11 efficiently inhibited the interaction of cortactin with F-actin. The mapping of the 4F11 epitope to the repeat region is consistent with the previous mapping of the F-actin binding sequence to the same region.

Regulation of the F-actin Binding Activity

Since tyrosine phosphorylation is an important posttranslational modification of cortactin in both transformed and mitogen-stimulated cells, we tested the effect of tyrosine phosphorylation on the binding of cortactin to F-actin (Fig. 10). Cell lysates from pp60^{src}-transformed CE cells were incubated with F-actin and subjected to sedimentation. The supernatant fraction (lanes *2S*) and the solubilized pellet fraction (lanes *2P* and *3P*) were immunoblotted with either phosphotyrosine antibodies (*a*) or mAb 4F11 (*b*). No cortactin was detected in the supernatant fraction by mAb 4F11 immunoblotting. To further test the partition of the tyrosine-phosphorylated cortactin, the supernatant fraction of a parallel sedimentation was immunoprecipitated with mAb 4F11 and the immunocomplex was blotted with either phosphotyrosine antibodies (*a*, lane *3S*) or mAb 4F11 (*b*, lane *3S*). The majority of the tyrosine-phosphorylated cortactin cosedimented with F-actin; no detectable tyrosine-phosphorylated cortactin was recovered from the supernatant fraction by anticortactin mAb immunoprecipitation (*a* and *b*, lanes *3S*). Since previous studies have shown that ~10–30% of cortactin is phosphorylated on tyrosine in pp60^{src}-transformed cells (Wu et al., 1991), we conclude that, within the limit of the assay used, tyrosine phosphorylation does not alter cortactin binding to F-actin.

Discussion

Remodeling of the cellular actin/cytoskeletal network occurs in response to a variety of extracellular and intracellular signals. In this paper we demonstrate that p80/85, a substrate for activated forms of pp60^{src}, other *src* family protein tyrosine kinases, and several growth factor receptor tyrosine kinases, is a filamentous actin-binding protein. p80/85, which we have termed cortactin, is present in multiple cell types and is enriched in the submembranous cortical region of adherent cells. The F-actin–binding region within cortactin maps to a domain comprised of five or six copies of a tandemly repeated sequence. Deletion of a highly conserved carboxyl-terminal SH3 domain, a structural motif common to many cytoskeleton-associated proteins, did not affect the binding of cortactin to F-actin. The F-actin–binding activity, its cortical localization, and tyrosine phosphorylation suggest that cortactin may play a role in mediating microfilament–membrane interactions in response to signals propagated by receptor and/or nonreceptor protein tyrosine kinases.

Cortactin Has a Specific, Saturable F-actin Binding Activity

Cortactin from three separate sources, i.e., CE cell lysates, programmed reticulocyte lysates or purified as a GST fusion protein from *E. coli*, bound specifically to polymerized actin in an F-actin cosedimentation assay. These data argue strongly for a direct interaction of cortactin with F-actin, and make it unlikely that the interaction with F-actin is mediated through another cellular protein present in the cortactin preparations. Although cortactin binds only to F-actin (not to monomeric actin; see below) and binds efficiently to purified actin from several sources, at present, we can not rule out the possibility that the binding to polymerized actin may be mediated by another F-actin–binding protein present in the actin preparations.

Using a GST–cortactin fusion protein produced in *E. coli*, we showed that the binding of cortactin to F-actin is saturable. We estimate that the stoichiometry of binding at saturation is ~1 GST.p80 protein per 14 actin monomers. A similar stoichiometry has been reported for other actin-binding proteins, such as brain α-actinin, macrophage actin-binding protein, and caldesmon (Pollard and Cooper, 1986). Analysis of the binding data yielded an apparent dissociation constant of $k_d = 0.43 \pm 0.08\ \mu M$, a value similar to that reported for the actin-binding protein spectrin, ABP 120, α-actinin, and MARCKS (Stossel et al., 1985; Hartwig et al., 1992). Removal of the GST portion of the GST.p80 protein by cleavage with thrombin increased the affinity of bacterially expressed cortactin for F-actin by approximately twofold (data not shown). To date, we have been unable to purify sufficient cortactin from CE cell lysates to perform kinetic measurements similar to those carried out with *E. coli*–

derived cortactin. Therefore it remains possible that post-translational modification of cortactin (serine/threonine phosphorylation, or tyrosine phosphorylation, see below) may directly alter the affinity or stoichiometry of cortactin binding to F-actin (Yamashiro et al., 1990; Hartwig et al., 1992).

The Repeat Region, but Not the SH3 Domain of Cortactin, Is Responsible for F-actin Binding

The evidence presented above indicates that the repeat region of cortactin is both required and sufficient for F-actin binding. The amino acid sequences comprising the individual repeats are highly conserved among each of the internal repeats (Fig. 1 *d*). Using both computer sequence analysis and visual inspection, we have been unable to identify sequence similarities with known actin-binding proteins or reported actin-binding sequences (Vanderkerckhove and Vancompernolle, 1992). However, analysis of the secondary structure of the individual tandem repeats predicts an α-helical region within the carboxyl-half of each repeat (Fig. 1 *d*). Computer modeling of the helical region revealed that the highly conserved lysine residues can be positioned on the same face of the predicted α-helix, contributing to a positively charged helical surface (data not shown). Such a lysine-rich helix has been reported in several actin-binding proteins (Friederick et al., 1992; Vanderkerckhove and Vancompernolle, 1992). Furthermore, the presence of the epitope for mAb 4F11 (a mAb that blocks actin binding and recognizes cortactin from avian, rodent, primate, and invertebrate species) in the repeat region suggests that this region of cortactin is likely to be exposed on the surface of the protein and may be available for protein–protein interaction.

Many F-actin–binding proteins also have monomeric actin-binding activity (Stossel et al., 1985; Pollard and Cooper, 1986). Cortactin was not retained on either a DNaseI affinity column or a DNaseI–actin affinity column, and thus does not appear to bind G-actin (data not shown).

Cortactin, present in several cell types, exhibits a characteristic colocalization with F-actin in the peripheral cortical region. In spite of its in vitro F-actin binding activity, little cortactin is observed to be associated with actin stress fibers. Several factors might explain the selective binding to cortical actin. For example, cortactin may bind specifically to an isoform of actin present in the cortical region or interact with an F-actin–binding protein present (or enriched) in the cell cortex. Alternatively, the presence of a membrane localization signal in cortactin may target cortactin to the submembranous region. The evidence discussed above shows that the carboxyl-terminal SH3 domain, a domain conserved in the *src* family of protein tyrosine kinases as well as in several proteins with diverse cellular functions (Pawson, 1988) is not directly involved in F-actin binding of cortactin. Several SH3-containing proteins associate either directly or indirectly with the plasma membrane, including myosin I, PLC-γ, spectrin, fodrin, dlgA, and NADPH oxidase-associated proteins (for review see Roadway et al., 1989). Thus the SH3 domain in cortactin may serve as a localization signal to link cortactin to integral or peripheral membrane proteins. Cortactin, together with the proposed SH3-binding proteins, may form complexes in the submembranous region, participating in the interaction of microfilaments with the plasma membrane.

Cortactin Is a Major Tyrosine-phosphorylated F-actin–binding Protein in pp60^{src} Transformed Cells

Previous studies have shown that cortactin becomes tyrosine phosphorylated to a high stoichiometry (~30% of the total cortactin) in pp60^{src}-transformed avian and rodent cells (Wu et al., 1991), as well as in cells stimulated with EGF, PDGF, and colony stimulating factor I (Downing and Reynolds, 1992; Maa et al., 1992). The data presented above indicate that tyrosine phosphorylation of cortactin does not influence F-actin binding. Therefore, the question remains how (if at all) tyrosine phosphorylation of cortactin might influence the actin remodeling observed in *src*-transformed cells. Previous studies have shown that cortactin codistributes with F-actin into podosomes in pp60^{src}-transformed cells (Wu et al., 1991). pp60^{src}-transformed cells, in comparison with untransformed cells, have a significant increase in the amount of actin in the Triton-insoluble cytoskeletal fraction (Holme et al., 1986). This partitioning of actin into the cytoskeletal fraction is correlated with a change in filamentous actin assemblies from "stress fiber" pattern to punctative filament aggregates, podosomes (Tarone et al., 1985; Marchisio et al., 1987). Although the molecular mechanism for the codistribution of cortactin with F-actin aggregates in transformed cells remains unclear, several possibilities can be entertained. There is growing evidence for specific and stable interaction between phosphotyrosine-containing proteins and proteins with SH2 domains. While many such proteins have specific catalytic functions (GTPase-activating protein for p21^{ras}, phospholipase C-γ, pp60^{src}), other proteins appear to function as "bridging" proteins (crk, SHC, and GRB2) (Mayer and Hanafusa, 1990; Cantley et al., 1991; Koch et al., 1991; Lowenstein et al., 1992; Pelicci et al., 1992). It is possible that tyrosine phosphorylation of cortactin may promote its binding to cellular proteins containing SH2 domains. Thus increased levels of tyrosine phosphorylation of cortactin may induce aberrant clustering/aggregation of cortactin–F-actin complexes with such proteins. Alternatively, tyrosine phosphorylation may affect the interaction of cortactin with F-actin by changing the binding affinity. Although such differences in binding have not been observed to date in our studies, the actin-binding properties of several proteins are affected by serine/threonine phosphorylation; e.g., MARCKS protein phosphorylated by protein kinase C and caldesmon phosphorylated by pp34^{cdc2} kinase both exhibit a decreased affinity to microfilaments (Yamashiro et al., 1990; Hartwig et al., 1992). Serine/threonine phosphorylation of cortactin is observed in normal and *src*-transformed cells and may be, along with tyrosine phosphorylation, an important regulatory signal (Wu et al., 1991).

Cortactin Has a Submembranous Localization in Cell Cortex

Indirect immunofluorescent staining of multiple cell types with anticortactin mAbs revealed a strong staining of the cortical structures such as membranous ruffles and lamellipodia. The actin network present in the cell cortex is a more transitory and dynamic structure in comparison with stress fibers. The structure, and in turn the mechanical properties of this actin network, is determined by the interaction of various classes of actin-binding proteins with actin. Several actin-binding proteins are reported to be enriched in the

cell cortex, including filamin, villin, gelsolin, and ezrin (Bretscher, 1991). Many of these proteins are also regulated by cellular signals, such as Ca^{2+}, phospholipids, and protein phosphorylation. The presence in the cell cortex of cortactin, an F-actin–binding protein that becomes tyrosine phosphorylated in response to ligand stimulation as well as in cellular transformation, makes cortactin an interesting candidate for a signal-transducing molecule or an effector molecule in the integration of extracellular stimulation with cytoplasmic changes. We note that cortactin is highly homologous to the product of EMS1, a gene located within the amplified chromosome 11q13 region in human carcinomas (Schuuring et al., 1992). The EMS1 gene product, therefore, may be the human counterpart of avian cortactin.

We thank S. J. Parsons, M. J. Weber, T. P. Bender, M. M. Smith, M. D. Schaller, D. C. Flynn, B. S. Cobbs, J. D. Hildebrand, J. L. Huff, T. A. Jamieson, and R. R. Vines for helpful comments on the manuscript and for discussions during the course of this work. We are particularly indebted to J. A. Cooper (Washington University, St. Louis) for his advice regarding the biochemistry of actin binding and C. A. Otey for providing an initial preparation of rabbit muscle actin. We thank G. Owens for providing rat smooth muscle and endothelial cells and D. C. Benjamin for computer modeling.

This work was supported by National Institute of Health grants CA29243 and CA40042.

Received for publication 2 October 1992 and in revised form 15 December 1992.

References

Albert, B., D. Bray, J. Lewis, M. Raff, K. Roberts, and J. D. Watson. 1989. The cytoskeleton. *In* Molecular Biology of the Cell. B. Albert, D. Bray, J. Lewis, M. Raff, K. Roberts, and J. D. Watson, editors. Garland Publishers, New York and London. 613–680.

Bray, D., J. Heath, and D. Moss. 1986. The membrane-associated "cortex" of animal cells: its structure and mechanical properties. *J. Cell Sci. Suppl.* 4:71–88.

Bretscher, A. 1991. Microfilament structure and function in the cortical cytoskeleton. *Annu. Rev. Cell Biol.* 7:337–374.

Cantley, L. C., K. R. Auger, C. Carpenter, B. Duckwirth, A. Graziani, R. Kapeller, and S. Soltoff. 1991. Oncogenes and signal transduction. *Cell.* 64:281–302.

Cooper, J. A. 1987. Effects of cytochalasin and phalloidin on actin. *J. Cell Biol.* 105:1473–1478.

David-Pfeuty, T., and S. J. Singer. 1980. Altered distribution of the cytoskeletal proteins vinculin and alpha actinin in cultured fibroblasts transformed by Rous sarcoma virus. *Proc. Natl. Acad. Sci. USA.* 77:6687–6691.

Davis, S., M. L. Lu, S. H. Lo, S. Lin, J. A. Butler, B. J. Druker, T. M. Roberts, Q. An, and L. B. Chen. 1991. Presence of an SH2 domain in the actin-binding protein tensin. *Science (Wash. DC).* 252:712–715.

Downing, J. R., and A. B. Reynolds. 1992. PDGF, CSF-1, and EGF induce tyrosine phosphorylation of p120, a $pp60^{src}$ transformation-associated substrate. *Oncogene.* 6:607–613.

Friederick, E., K. Vancompernolle, H. Christian, M. Goethals, J. Finidori, J. Vandekerckhove, and D. Louvard. 1992. An actin-binding site containing a conserved motif of charged amino acid residues is essential for the morphogenic effect of villin. *Cell.* 70:81–92.

Glenney, J. R., and L. Zokas. 1989. Novel tyrosine kinase substrates from Rouse sarcoma virus-transformed cells are present in the membrane skeleton. *J. Cell Biol.* 108:2401–2408.

Goldschmidt-Clermont, P. J., J. M. Kim, L. M. Machesky, S. G. Rhee, and T. D. Pollard. 1991. Regulation of phospholipase C-γ1 by profilin and tyrosine phosphorylation. *Science (Wash. DC).* 251:1231–1233.

Hamaguchi, M., and H. Hanafusa. 1987. Association of $pp60^{src}$ with Triton X-100-resistant cellular structure correlates with morphological transformation. *Proc. Natl. Acad. Sci. USA.* 84:2312–2316.

Hartwig, J. H., and D. J. Kwiatkowski. 1991. Actin-binding proteins. *Curr. Opin. Cell Biol.* 3:87–97.

Hartwig, J. H., M. Thelen, A. Rosen, P. A. Janmey, A. C. Nairn, and A. Aderem. 1992. MARCKS is an actin filament cross-linking protein regulated by proteins kinase C and calcium-calmodulin. *Nature (Lond.).* 356:618–622.

Holme, T. C., S. Kellie, J. A. Wyke, and N. Crawford. 1986. Effect of transformation by Rous sarcoma virus on the character and distribution of actin in Rat-1 fibroblasts: a biochemical and microscopical study. *Br. J. Cancer.* 53:465–476.

Hug, C., T. M. Millers, M. A. Torres, J. F. Casella, and J. A. Cooper. 1992. Identification and characterization of an actin-binding site of CapZ. *J. Cell Biol.* 116:923–931.

Hunter, T. 1989. Protein modification: phosphorylation on tyrosine residues. *Curr. Opin. Cell Biol.* 1:1168–1181.

Jove, R., and H. Hanafusa. 1987. Cell transformation by the viral *src* oncogene. *Annu. Rev. Cell Biol.* 3:31–56.

Kanner, S. B., A. B. Reynolds, and J. T. Parsons. 1991*a*. Tyrosine phosphorylation of a 120-kilodalton $pp60^{src}$ substrate upon epidermal growth factor and platelet-derived growth factor receptor stimulation and in polyomavirus middle-T-antigen-transformed cells. *Mol. Cell Biol.* 11:713–720.

Kanner, S. B., A. B. Reynolds, H-C. R. Wang, R. R. Vines, and J. T. Parsons. 1991*b*. The SH2 and SH3 domains of $pp60^{src}$ direct stable association with tyrosine-phosphorylated proteins p130 and p110. *EMBO (Eur. Mol. Biol. Organ.) J.* 10:1689–1698.

Koch, C. A., D. Anderson, M. F. Moran, C. Ellis, and T. Pawson. 1991. SH2 and SH3 domains: elements that control interaction of cytoplasmic signalling proteins. *Science (Wash. DC).* 252:1564–1570.

Laemmli, U. K. 1970. Cleavage of structural proteins during the assembly of the head of bacteriophage T4. *Nature (Lond.).* 227:680–685.

Lowenstein, E. J., R. J. Daly, A. G. Batzer, W. Li, B. Margolis, R. Lammers, A. Ullrich, and J. Schlessinger. 1992. The SH2 and SH3 domain-containing protein GRB2 links receptor tyrosine kinases to ras signalling. *Cell.* 70: 431–442.

Maa, M-M., L. K. Wilson, J. S. Moyers, R. R. Vines, J. T. Parsons, and S. J. Parsons. 1992. Identification and characterization of a cytoskeleton-associated, epidermal growth factor sensitive $pp60^{src}$ substrate. *Oncogene.* 7:2429–2438.

Marchisio, P. C., D. Cirillo, A. Zamborin-Zallone, and G. Tarone. 1987. Rous sarcoma virus-transformed fibroblasts and cells of monocytic origin display a peculiar dot-like organization of cytoskeletal proteins involved in microfilament-membrane interaction. *Exp. Cell Res.* 169:202–214.

Mayer, B. J., and H. Hanafusa. 1990. Association of the *v-crk* oncogene product with phospho-tyrosine-containing protein kinase activity. *Proc. Natl. Acad. Sci. USA.* 86:2638–2642.

Neri, A., C-C. Chang, L. Lombardi, M. Salina, P. Corradin, A. T. Maiolo, R. S. K. Chaganti, and R. Dalla-Farvera. 1991. B cell lymphoma-associated chromosomal translocation involves candidate oncogene *lyt-10*, homologous to NF-κB p50. *Cell.* 67:1075–1087.

Noegel, A. A., and M. Schleicher. 1991. Phenotypes of cells with cytoskeletal mutations. *Curr. Opin. Cell Biol.* 3:18–26.

Pardee, J. D., and J. A. Spudich. 1982. Purification of muscle actin. *Methods Enzymol.* 85:164–181.

Parsons, J. T., and M. J. Weber. 1989. Genetics of *src*: structure and function of a protein tyrosine kinase. *Curr. Top. Microbiol. Immunol.* 147:79–127.

Pawson, T. 1988. Non-catalytic domains of cytoplasmic protein-tyrosine kinases: regulatory elements in signal transduction. *Oncogene.* 3:491–495.

Pelicci, G., L. Lanfrancone, F. Grignani, J. McGlade, F. Cavall, G. Firni, I. Nicoletti, F. Grignani, T. Pawson, and P. G. Pelicci. 1992. A novel transforming protein (SHC) with an SH2 domain is implicated in mitogenic signal transduction. *Cell.* 70:93–104.

Pollard, T. D., and J. A. Cooper. 1986. Actin and actin-binding proteins. A critical evaluation of mechanisms and functions. *Annu. Rev. Biochem.* 55: 987–1035.

Pope, B., and A. G. Weeds. 1986. Binding of pig plasma gelsolin to F-actin and partial fractionation into calcium-dependent and calcium-independent forms. *Eur. J. Biochem.* 161:85–93.

Reynolds, A. B., J. Rossel, S. B. Kanner, and J. T. Parsons. 1989. Transformation-specific tyrosine phosphorylation of a novel cellular protein in chicken cells expressing oncogenic variants of the avian cellular *src* gene. *Mol. Cell Biol.* 9:629–638.

Reynolds, A. B., L. Herbert, J. L. Cleveland, S. T. Berg, and J. R. Gaut. 1992. P120, a novel substrate of protein tyrosine kinase receptors and of $p60^{src}$, is related to cadherin-binding factors, β-catenin, plakoglobin and *armadillo*. *Oncogene.* 7:2439–2445.

Rodaway, A. R., M. J. Sternberg, and D. L. Bentley. 1989. Similarity in membrane proteins. *Nature (Lond.).* 342:624.

Rothberg, K. G., J. E. Henser, W. C. Donzell, Y-S. Ying, J. R. Glenney, and R. G. W. Anderson. 1992. Caveolin, a protein component of caveolae membrane coats. *Cell.* 68:673–682.

Schaller, M. D., C. A. Borgman, B. J. Cobb, R. R. Vines, A. B. Reynolds, and J. T. Parsons. 1992. $pp125^{FAK}$, a structurally distinctive protein-tyrosine kinase associated with focal adhesions. *Proc. Natl. Acad. Sci. USA.* 89:5192–5196.

Schaller, M. D., A. H., Bouton, D. C. Flynn, and J. T. Parsons. 1993. Identification and characterization of novel substrates for protein tyrosine kinases. *Proc. Nucleic Acid Res. Mol. Biol.* In press.

Schuuring, E., E. Verhoeven, W. J. Mooi, and R. J. A. M. Michalides. 1992. Identification and cloning of two overexpressed genes, U21B31/PRAD1 and EMS1, within the amplified chromosome 11q13 region in human carcinomas. *Oncogene.* 7:355–361.

Small, J. V., G. Rinnerthaler, and H. Hinssen. 1981. Organization of actin meshworks in cultured cells: the leading edge. *Cold Spring Harbor Symp. Quant. Biol.* 46:599–611.

Smith, D. B., and K. S. Johnson. 1988. Single-step purification of polypeptide expressed in *Escherichia coli* as fusions with glutathione S-transferase. *Gene*

(*Amst.*). 67:31–40.
Stossel, T. P. 1989. From signal to pseudopod. *J. Biol. Chem.* 264:18261–18264.
Stossel, T. P., J. H. Hartwig, H. L. Yin, K. S. Zaner, and O. I. Standadl. 1981. Actin gelation and the structure of cortical cytoplasm. *Cold Spring Harbor Symp. Quant. Biol.* 46:567–578.
Stossel, T. P., C. Chaponnier, R. M. Ezzell, J. H. Hartwig, P. A. Janmey, D. J. Kwiatkowski, S. E. Lind, D. B. Smith, F. S. Southwick, H. L. Yin, and K. S. Zaner. 1985. Nonmuscle actin-binding proteins. *Annu. Rev. Cell Biol.* 1:353–402.
Tarone, G., D. Cirrillo, F. G. Giancotti, P. M. Comoglio, and P. C. Marchisio. 1985. Rous sarcoma virus-transformed fibroblasts adhere primarily at discrete protrusions of the ventral membrane called podosomes. *Exp. Cell Res.* 159:141–157.
Tilney, L. G. 1983. Interaction between actin filaments give spatial organization to cells. *Mod. Cell Biol.* 2:163–199.
Turner, C. E., J. R. Glenney, and K. Burridge. 1990. Paxillin: a new vincullin-binding protein present in focal adhesions. *J. Cell Biol.* 111:1059–1068.
Vandekerckhove, J. 1990. Actin-binding proteins. *Curr. Opin. Cell Biol.* 2:41–50.
Vanderkerckhove, J., and J. Vancompernolle. 1992. Structural relationships of actin-binding proteins. *Curr. Opin. Cell Biol.* 2:36–42.
Wong, S., A. B. Reynolds, and J. Papkoff. 1992. Platelet activation leads to increased c-*src* kinase activity and association of c-*src* with an 85-kDa tyrosine phosphoprotein. *Oncogene.* 7:2407–2415.
Wu, H., A. B. Reynolds, S. B. Kanner, R. R. Vines, and J. T. Parsons. 1991. Identification of a novel cytoskeleton-associated $pp60^{src}$ substrate. *Mol. Cell Biol.* 11:5113–5124.
Yamashiro, S., Y. Yamakita, R. Ishikawa, and F. Matsumura. 1990. Mitosis-specific phosphorylation causes 83K non-muscle caldesmon to dissociate from microfilaments. *Nature (Lond.).* 344:675–678.